Stress path triaxial tests for a deep open cut excavation

Tests triaxiaux de trajectoire de stress pour une excavation à découpe profonde

Jeong-Yun Won
Senior Geotechnical Engineer, Barr Engineering Co., USA, jeongyun.won@gmail.com

Blake Cotton
Principle Engineer, GeoEngineers, USA

ABSTRACT: A deep open cut excavation in Pleistocene overconsolidated clay was considered for a river diversion channel. A stress path testing program was carried out to investigate effects of the stress changes on deformation and shear strength of the clay. Total and effective stress changes in vertical and horizontal directions were replicated by actively controlled axial loads, cell pressures and back pressures. Undrained and drained shear strengths from the stress path testing were significantly different from the conventional K_o-consolidated triaxial tests. Complex directional deformations were observed during the stress paths. The stress path approach is an attractive method to investigate soil behaviors for slope stability problems in clay.

RÉSUMÉ: Une excavation en profondeur ouverte dans l'argile sur-consolidée du Pléistocène a été envisagée pour un canal de dérivation de rivière. Un programme d'essais de contraintes a été réalisé pour étudier les effets des changements de contraintes sur la déformation et la résistance au cisaillement de l'argile. Les changements de contraintes totales et effectives dans les directions verticales et horizontales ont été répliqués par des charges axiales activées, des pressions cellulaires et des contre-pressions. Les forces de cisaillement non drainées et drainées du test de trajectoire de contrainte étaient significativement différentes des essais triaxiaux de Ko-consolidés classiques. Des déformations directionnelles complexes ont été observées pendant les trajets de contraintes. L'approche du chemin de stress est une méthode attrayante pour étudier les comportements du sol pour des problèmes de stabilité des pentes dans l'argile.

KEYWORDS: Stress-path, clay, excavation, slope stability, shear strength, triaxial test

1 INTRODUCTION

A deep open cut excavation of 24-29 m in overconsolidated clay was considered for a river diversion channel in Louisiana, USA. The man-made channel would divert a body of water to reduce flooding risks of the nearby areas. At the early stage of the plan, critical geotechnical concerns were raised regarding the short- and long-term slope stabilities. The concerns included potential swelling, weathering and strength reduction during excavation and operation.

Slope stability of cut slopes in overconsolidated clay has been one of the geotechnical challenges over the last few decades. Numerous slopes failed long after the completion of the cut. Many geotechnical studies have focused on delayed failure, progressive failure and fully softened shear strength. Delayed failure mechanism can be summarized as a failure that was delayed by the slow rate of increase in pore pressure from negative excess pore pressure and a decrease in shear strength (Vaughan and Walbancke 1973, Mesri *et al.* 1978). Progressive failure mechanism was investigated by Skempton (1964) and Pott *et al.* (1997). Fully softened shear strength was introduced by Skempton (1964, 1970) for first-time slides in mainly overconsolidated clays. Mesri and Shahien (2003) found that the fully softened shear strength is the lower bound for mobilized strength in first-time slope failures and part of the slip surface may be at the residual condition. The previous studies demonstrate that the main challenges are (1) understanding and estimating appropriate shear behaviors for a given clay and (2) modelling future field conditions such as failure modes, pore pressure increases and shear strength decreases with time.

As an alternative method to the previous approaches, a laboratory stress path testing program was proposed to investigate shear behaviors of the clay deposit due to the planned excavation. Since the stress path method was introduced (Lambe and Marr 1979), significant developments have been made, including advances in testing equipment and various applications of the stress path method. Hird and Pierpoint (1997) and Won *et al.* (2014) attempted to investigate mobilized shear strengths and deformation behaviors of clay soils specifically in open cut excavations by the stress path method.

This paper presents a stress path testing program performed during the early planning stage of the river diversion project to investigate effects of the stress changes on deformation and shear strength of the overconsolidated clay along the cut slope. To cover various stress changes at different locations of the slope, 34 stress path tests were performed. Stress changes that can occur during construction and operation stages were applied on undisturbed specimens in triaxial conditions. In the stress path tests, axial loads, cell pressures and back pressures were actively and independently controlled to implement the planned stress paths. Part of the test results, representing the crest, near toe and base of the slope are presented. Stress path results are compared with the conventional K_o-consolidated triaxial compression and extension tests. Undrained and drained shear strengths as well as deformation behaviors are discussed.

2 STRESS CHANGES DUE TO EXCAVATION

Lambe (1970) provided key aspects that can occur in soil elements near an excavation, i.e., the stress changes are related to the reductions in total vertical and horizontal stresses, followed by the changes in equilibrium pore pressure. Bolton (1993) illustrated stress changes at the base of an excavation and suggested that the clay would behave like an undrained triaxial extension test (reducing vertical stress with a constant horizontal stress). Won *et al.* (2014) presented examples of stress changes at different locations along an excavation slope.

Soil elements around an excavation, e.g., Point A, B and C shown in Figure 1 will experience a series of stress changes in total and effective stresses as a result of the excavation. Soil element at Point A will experience a total horizontal stress (σ_h)

decrease during the first excavation stage. The total vertical stress (σ_v) at Point A, however, remains unchanged during this stage. Soil element at Point B will experience total vertical stress (σ_v) decreases during the staged excavations whereas the total horizontal stress (σ_h) remains the same. Soil element at Point C will have more complex stress changes as it experiences total vertical stress (σ_v) decreases followed by a total horizontal stress (σ_h) decrease during the fourth excavation stage. Ground water level and pore pressure changes around the cut slope will make the stress changes even more complicated.

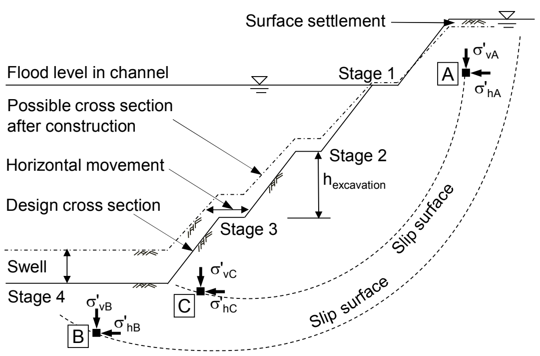

Figure 1. Schematic cross section of an open cut excavation.

Pore pressures (u) at the soil elements along the slope will partially decrease and increase during the staged excavation and swelling (waiting) stages. For example, at Point B, an excavation stage can be considered as undrained extension because this stage typically lasts short time. This total vertical stress decrease will generate a negative excess pore pressure. The negative excess pore pressure (u′) will increase the effective stresses and, in turn, shear strength of the soil. The slope at this stage (short-term) is typically stable by this negative excess pore pressure.

After the excavation stage is over, either during a waiting period in a staged cut or by the end of construction, the soil elements will experience additional stress changes with time due to pore pressure changes. The negative excess pore pressure starts to dissipate leading to an increase in the pore pressure, which in turn, leads to a decrease in the effective stresses. This decrease in effective stresses will decrease the shear strength, which may result in an unstable slope. Furthermore, in an open cut excavation, deformations, e.g., swell, would impact the mobilized shear strengths as a result of stress changes. Any modifications, such as further excavation, a prolonged drought or flooding can cause an undrained or drained loading condition.

Table 1. Stress changes during stress path testing for Point C.

	σ_v (kPa)	σ_h (kPa)	u (kPa)	σ'_v (kPa)	σ'_h (kPa)
Ko-consolidation	475	-	244	231	-
1st excavation	354	341	155	199	186
1st swell (waiting)	352	307	184	168	123
2nd excavation	236	307	95	141	212
2nd swell (waiting)	237	277	124	113	153
3rd excavation	119	250	35	84	215
3rd swell (waiting)	118	250	64	54	186
4th excavation	121	81	64	57	17
Water level rise	241	199	184	57	15

In Table 1, as an example, stress changes at Point C are summarized for each step of construction and operation. In fact, the stress values in the table were assigned as target stresses during a stress path test. A numerical analysis can estimate stress changes along the slope, considering stress-strain behavior, construction sequence, seepage, volume changes and progressive failure modes. This study, however, used analytically calculated stress changes for the stress path testing. Values for the total and effective vertical and horizontal stresses at each stage of the excavation were determined with assumed pore pressure responses due to the total stress changes. The main focus was to investigate deformation behaviors and shear strength changes due to the stress changes associated with the excavation for the given clay layers.

3 TEST MATERIALS AND STRESS PATH TESTING

The Pleistocene clayey layers (CL and CH), adjacent to the Mississippi River in Louisiana, USA, have numerous thin sublayers of silt and sand, and abundant slickensides. Fixed piston samplers of 127 mm (5-in) diameter and 1.47 m (54-in) long were used to retrieve continuous undisturbed samples during the site investigation program. Multiple cut sections (127 mm in diameter and 300 mm long) were collected from the sampling tubes and coated by paraffin for storage. Triaxial test specimens of nominal diameter of 50 mm and height of 120 mm were trimmed from the cut sections. Natural moisture contents of the tested samples ranged from 18 to 55 % and were generally close to their plastic limits (12 to 30 %). Coefficient of earth pressure at rest, K_o values measured during K_o-consolidation stages ranged mostly between 0.4 and 0.7. Oedometer tests were performed on 100 mm diameter undisturbed specimens. Overconsolidation ratios from the oedometer tests ranged between 3 and 5.

After back pressure saturation, the specimens were consolidated to their estimated in-situ effective vertical stresses in K_o-state, following the recompression concept (without any loading-unloading stages). Then, each stress path step was implemented by manually controlling the three (3) pressure units – axial load, cell pressure and back pressure – so that each pressure can be controlled independently and simultaneously. The specimens were allowed to deform axially and radially during the stress paths. The deformations were monitored by a vertical displacement sensor and the volume changes in the pressure controllers. The stress paths were followed by an undrained shear in compression or extension, depending on the locations of the specimens with respect to the slope. More details about the stress path testing were described by Won *et al.* (2014).

Each stress path testing had a companion K_o-consolidated compression or extension test. In most cases, specimens for the companion tests were trimmed from the same cut section. Point A had a CIUC (isotropically consolidated undrained compression) and a CK_oUC (K_o-consolidated undrained compression) triaxial tests in addition to the stress path tests. Two (2) types of extension test, i.e., CK_oUE1 and CK_oUE2 were also performed. CK_oUE1 represents a K_o-consolidated extension test, where the axial load was decreased while the cell (chamber) pressure was maintained constant. In CK_oUE2, the cell pressure was increased while the axial load was maintained constant.

4 RESULTS AND DISCUSSION

Stress path test results for Point A, B and C are presented in terms of effective stresses in Figure 2, Figure 3 and Figure 4, respectively. Natural water content (W_n), liquid limit (LL) and plasticity index (PI) values of the tested specimens are presented in the plots. Companion triaxial test results (CIUC, CK_oUC, CK_oUE1 and CK_oUE2) are also presented in the p'-q plots. Mean effective stress, p' is defined as ½ ($\sigma'_v + \sigma'_h$) and deviator stress, q is equal to ½ ($\sigma'_v - \sigma'_h$). Since the major principle stresses (σ'_1 and σ'_3) constantly changed during the stress paths and triaxial extension tests, effective vertical (axial) and effective horizontal (radial) stresses are used and denoted as σ'_v and σ'_h, respectively. Failure points were selected based on the maximum obliquity (σ'_v/σ'_h) criterion. Secant effective friction angles (ϕ'_s) were determined based on an assumption that the effective cohesion is zero. The starting points of the tests were different because of the different stress conditions after the K_o consolidation stages.

The stress paths assigned for Point A (open squares in Figure 2) initially decreased p' for the first excavation stage, followed by increases in p' and q. The specimen for Point A went through a drought condition (constant σ_v and σ_h with decreased u) before the undrained shear in compression. The resulting failure point (diamond in Figure 2) has a secant friction angle (ϕ'_s) of 36.4 degrees that is higher than the CIUC (triangle in Figure 2) and CK_oUC (circle in Figure 2) results. The high undrained shear strength in compression from the stress path test seems to be mobilized by the high p' value during the drought condition.

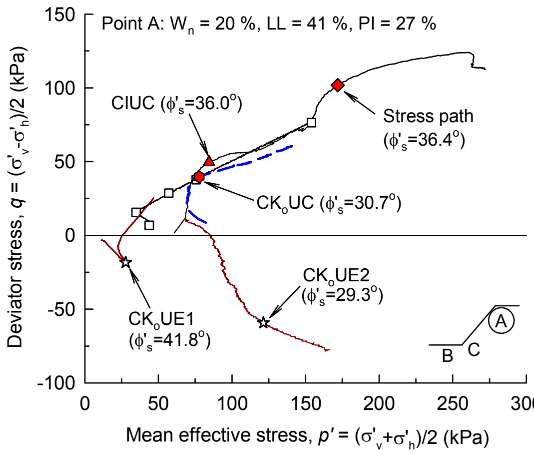

Figure 2. Stress path and triaxial test results for Point A.

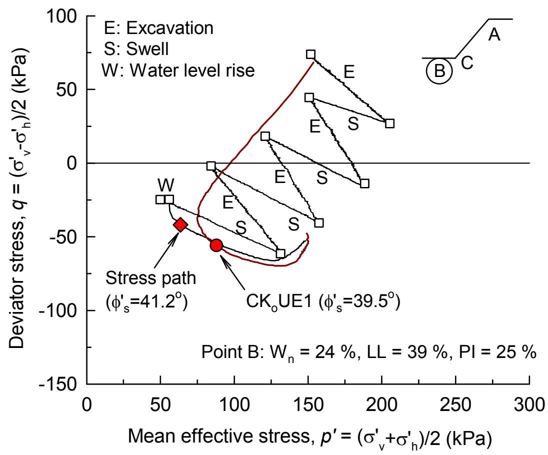

Figure 3. Stress path and CKoUE1 test results for Point B.

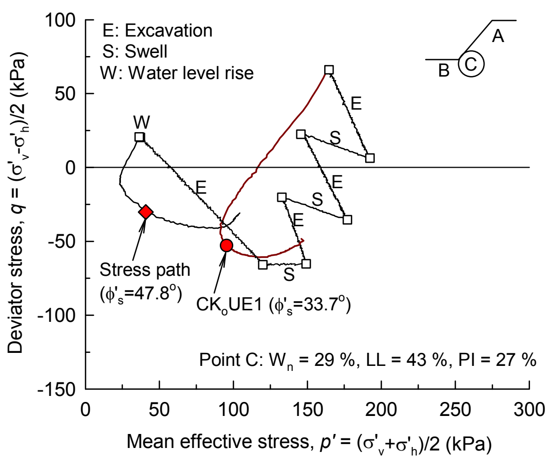

Figure 4. Stress path and CKoUE1 test results for Point C.

The CK_oUE1 and CK_oUE2 performed on the companion specimens showed significantly different shearing behaviors (Figure 2). The secant friction angle (ϕ'_s) from CK_oUE1 is higher whereas the undrained shear strength at failure is significantly lower than CK_oUE2. A line can be drawn through the two failure points (stars in Figure 2), constructing a unique failure envelope for the given clay. Instead of having two extension shear modes, CK_oUE1 was selected as the representative undrained shear mode at the end of stress paths.

The stress paths assigned for Point B, shown in Figure 3, had multiple stages representing excavation and swelling stages, followed by a water level rise stage. The water level rise (flooding of the diversion channel) stage was modelled as an undrained load in which the effective stresses remained the same while the total stresses were increased. The undrained shear in extension after 9 steps of the stress paths for Point B shows a secant friction angle (ϕ'_s) of 41.2 degrees. A companion specimen from CK_oUE1 shows a slightly lower secant friction angle (ϕ'_s=39.5 degrees) whereas the undrained shear strength at failure is higher.

The specimen for Point C, shown in Figure 4, experienced similar stress paths as Point B until the last excavation stage. During the last excavation stage, the total horizontal stress (σ_h) was decreased whereas the total vertical stress (σ_v) remained the same. This condition is similar to the first step of Point A, resulting in a positive q in Figure 4. The specimen experienced a water level rise stage before the undrained shear in extension. A very high secant friction angle (ϕ'_s=47.8 degrees) is shown from the undrained shear in extension after the stress paths, assuming a zero cohesion. A companion specimen for CKoUE1 shows a moderate secant friction angle (ϕ'_s=33.7 degrees) whereas the undrained shear strength at failure is higher than the stress path. It should be emphasized that the individual secant effective friction angles with zero effective cohesion shown in the figures are for comparison purposes only and should not be interpreted as actual shear strength parameters.

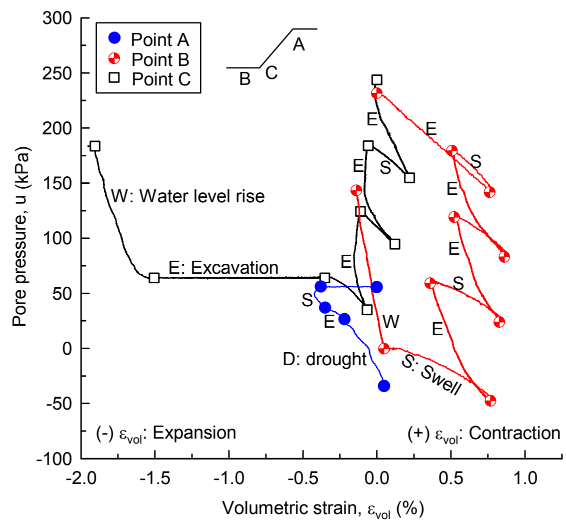

Figure 5. Volumetric strains during the stress paths.

Volumetric strains (ε_{vol}) throughout the stress paths for the three (3) specimens are presented in Figure 5. The actively controlled pore pressures (u) considered the hydrostatic pore pressures (before and during the excavation) and the excess pore pressures at any given time. For Points B and C, the pore pressures were assigned to decrease during the excavation stages (i.e., negative excess pore pressure) then to recover partially during the waiting time. During the flooding event, the pore pressures were increased in response to the increased water level. It should be noted that the volumetric strains are combinations of vertical (axial) and horizontal (radial) strains; in other words they represent combined changes in specimen height and diameter. The positive strain is for contraction (decrease in volume) and the negative strain is for expansion (increase in volume).

Given the stress paths, the volumetric strains responded to the effective vertical and horizontal stresses within a narrow range between +0.7 and -0.5 %. As Won *et al.* (2014) pointed out, the clay samples at the site did not exhibit a high swelling potential. Vertical and horizontal strains may develop to the opposite directions during a given stress path, as reported by Won *et al.* (2014). The most distinctive volume change among the results shown in Figure 5 is the one during the last excavation stage near the toe (Point C). During the last excavation stage, the specimen for Point C exhibited a compressive vertical strain (decrease in height) whereas the horizontal strain moved to the negative direction (increase in diameter, expansion), resulting in a net increase in volume (expansion, negative). This substantial volume change, especially the horizontal expansion near the toe implies that the slope will experience progressive deformations at the toe. The progressive deformations would propagate stress concentrations and may lead to a progressive failure.

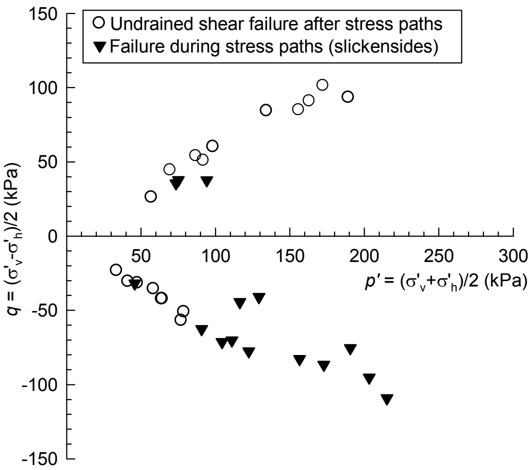

Figure 6. Failure points from stress path tests.

Failure points, based on the maximum obliquity (σ'_v/σ'_h) criterion, from 34 stress path tests are presented in Figure 6. One (1) failure point from a silt specimen is not shown. Prematurely failed specimens – failed along the slickensides that were about 40 % of the tested specimens (Won *et al.* 2014) – are also presented as failure points. The premature failures during the stress paths are indeed strong indications of failures that can occur during the excavation or operation. The failure points include the specimens from CL and CH materials and the specimens experienced various stress paths, thus they may or may not validate a single linear failure envelope for the project. Furthermore, different failure criteria will produce different failure points for the same test set. Failure points grouped by its consistency, stress path patterns or locations along the cut slope would provide pertinent failure envelopes that reflect realistic stress histories and volume changes in the field. Fully softened shear strengths were not investigated as part of the study, thus a comparison is not available at the time of this paper.

The most common slope stability analysis method, limit equilibrium analysis, is mainly based on an assumption that the shear strengths along the potential slip surface mobilize simultaneously, regardless of its strain or stress level (Duncan and Wright 2005). The stress path results presented in this paper demonstrate that the soil elements along the excavation slope will undergo complex stress paths and volume changes, and will mobilize different undrained and drained shear strengths. Undrained shear strengths from the conventional CK_oUE tests can be significantly overestimated, based on the comparison with the stress path results. Long-term slope stability will be governed by effective stress conditions as the pore pressure changes with time. Effective shear strength parameters, such as effective friction angle and effective cohesion could be estimated by the failure points from the stress path testing. The high secant friction angles (ϕ'_s) from the individual stress path results with zero effective cohesion are unrealistic but still provide value for comparison purposes. Effective friction angles with moderate effective cohesions will be more reasonable for stability analyses. The mobilized undrained and drained shear strengths from the stress path testing show the stress path dependency of the clay. The stress path approach provides an attractive method for determining short- and long-term stabilities of cut slopes, because it considers stress changes at different locations, reflects pore pressure changes and realizes volume changes. Because of the complex geological features of the site and the scope of the testing program, no attempts were made to develop any shear strength parameters.

5 CONCLUSIONS

A series of stress path tests for an open cut excavation was carried out to investigate effects of the stress changes on deformation and shear strengths of the overconsolidated clay. The following summarizes the findings of the study.

- Undrained shear strengths from the stress path tests for the toe and base of the cut slope are substantially lower than those from the conventional K_o-consolidated undrained triaxial extension tests.
- Complex deformations in vertical and horizontal directions were observed from the stress path tests. The volume changes were mainly governed by the effective stress changes.
- Effective strength parameters can be estimated by the failure points from the stress path testing.
- Stress path testing is an attractive method to investigate soil behaviors for short- and long-term slope stabilities.

6 REFERENCES

Bolton M.D. 1993. Mechanisms of ground deformation due to excavation in clay. Excavation in Urban Areas, Adachi, T. ed., *Japanese Society Soil Mechanics and Foundation Engineering*, Japan, 1-33.

Duncan J.M. and Wright S.G. 2005. *Soil Strength and Slope Stability*. John Wiley & Sons, Inc.

Hird C.C. and Pierpoint N.D. 1997. Stiffness determination and deformation analysis for a trial excavation in Oxford Clay. *Geotechnique* 47 (3), 665-691.

Lambe T.W. 1970. Braced excavation. *Proc. Specialty Conf. Lateral Stresses in the Ground and Design of Earth-Retaining Structures*, ASCE, 149-218.

Lambe T.W. and Marr W.A. 1979. Stress path method: Second edition. *J. Geotech. Eng. Div.* 105 (GT6), 727-738.

Mesri G. and Shahien M. 2003. Residual shear strength mobilized in first-time slope failures. *J. Geo. & Geoenv. Eng.* 129 (1), 12-31.

Mesri G., Ulrich C.R., and Choi Y.K. 1978. The rate of swelling of overconsolidated clays subjected to unloading. *Geotechnique* 28 (3), 281-307.

Pott D.M., Kovacevic N., and Vaughan P.R. 1997. Delayed collapse of cut slopes in stiff clay. *Geotechnique* 47 (5), 953-982.

Skempton A.W. 1964. Long-term stability of clay slopes. *Geotechnique* 14 (2), 77-101.

Skempton A.W. 1970. First-time slides in over-consolidated clays. *Geotechnique* 20 (3), 320-324.

Vaughan P.R. and Walbancke H.J. 1973. Pore pressure changes and the delayed failure of cutting slopes in overconsolidated clay. *Geotechnique* 23 (4), 531-539.

Won J.Y., Cotton B., and Porter B.W. 2014. Deformation and shear strength behaviors of overconsolidated clay from stress-path testing for a deep open cut excavation. *From Soil Behavior Fundamentals to Innovations in Geotechnical Eng.,* ASCE GSP 233, 388-399.